

## **Experimental and Thermodynamic Assessment of Beryllium-Replacement Materials for CANDU<sup>®</sup> Brazed Joints**

**K.N. Potter<sup>1</sup>, G.A. Ferrier<sup>1</sup>, F.C Dimayuga<sup>2</sup> and E.C. Corcoran<sup>1</sup>**

<sup>1</sup>Royal Military College of Canada, Kingston, Ontario, Canada  
(Kieran.Potter@rmc.ca)

<sup>2</sup>Canadian Nuclear Laboratories, Chalk River, Ontario, Canada

*Note: A condensed version of this paper has been submitted to the parallel  
39<sup>th</sup> CNS/CNA Student Conference to be presented as a poster.*

### **Abstract**

Currently, appendages are joined to CANDU<sup>®</sup> fuel elements via a brazing process, with beryllium as the filler material. A potential reduction in the occupational limit on airborne beryllium particulates has motivated research into alternative brazing materials. To this end, the Canadian nuclear industry has funded an initiative to identify and evaluate the suitability of several candidate brazing materials.

This work describes contributions toward the assessment of alternative brazing materials from the Royal Military College of Canada (RMCC). An impact testing method was developed to evaluate the mechanical strength of candidate braze joints. Thermodynamic modelling was performed to predict the aqueous behaviour of each candidate material in CANDU coolant conditions characteristic of reactor shutdown, and corrosion experiments are underway to support modelling predictions. The results of these activities will assist in selecting a suitable replacement material for beryllium.

### **1. Introduction**

CANDU fuel sheaths feature two types of appendages: spacers and bearing pads. Spacers are small Zircaloy-4 (Zr-4) pieces, which are attached at the axial centre of each fuel element. The spacers ensure that separation between fuel elements is maintained [1]. Larger Zr-4 appendages called bearing pads are attached to the exterior elements of the fuel bundle. These allow the bundle to slide within the pressure tube and maintain the designed geometry of the bundle within the fuel channel. Specifically, they position the fuel bundles such that the fuel sheaths do not contact the pressure tube, thereby allowing the heat transport system to work effectively. Both appendages are shown in Figure 1.

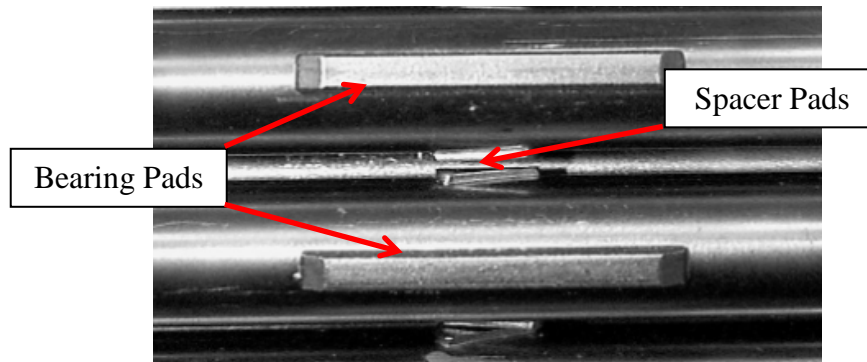


**Figure 1-Bearing pads and spacers attached to fuel sheathing [1].**

These appendages are attached to fuel sheaths using a brazing process, with beryllium (Be) as the filler material. This process can create airborne beryllium oxide particulates, which are a health hazard to workers in the manufacturing environment. To address this concern, the Ontario Ministry of Labour is expected to adopt a 40-fold reduction in the allowable limit on airborne Be particulates [2]. This could interfere with CANDU fuel manufacturing, as current methods may have difficulty achieving compliance with the new regulations. In anticipation of this change, a CANDU Owners' Group (COG) initiative has been launched to investigate the use of alternative filler materials to replace beryllium [3]. Within this initiative, extensive testing of alternative material brazed joints is required. This includes evaluations of joint constructability, mechanical strength, corrosion resistance, high temperature behaviour, and behaviour under irradiation.

The present work focuses on evaluating the impact strength and corrosion resistance of alternative material brazed joints. A testing method was designed and experiments were performed to assess the impact strength of alternative material brazed joints, as compared to existing Be joints. Thermodynamic modelling was undertaken to generate predictions of corrosion susceptibility for the brazing materials under consideration. Additionally, experiments are underway to supplement modelling predictions and assess the suitability of each candidate material based upon corrosion behaviour in coolant conditions characteristic of reactor shutdown. The results of these studies will assist in determining the most promising brazing material.

## **2. Impact Testing**

During refuelling operations, high loading rate forces may be imposed upon appendage braze joints. Any potential replacement brazing material must produce joints that are able to withstand these forces. Consequently, a testing method was developed to measure the impact strengths of joints brazed with various candidate materials. A candidate material is considered promising if it forms brazed joints that exhibit impact strengths greater than or equal to the impact strengths of beryllium-brazed joints. This criterion is an important component of the COG assessment of suitable replacement brazing materials.

### **2.1 Test Methodology**

An impact testing method based upon the Izod pendulum impact test (ASTM D256) was developed for evaluating the impact strength of CANDU brazed joints [4]. This method uses a striking hammer

fastened to the distal end of a weighted pendulum. Individual sheath sections with brazed bearing pads are clamped in place within a specialized sample holder such that the striking hammer will impact the pad just above the joint, breaking it off of the sheath. The energy loss of the pendulum is calculated based on the difference between its initial height and upswing height, according to Equation 1:

$$\Delta E = mg\Delta H \quad (1)$$

where  $\Delta E$  is the energy lost,  $m$  is the mass of the pendulum,  $g$  is the gravitational acceleration, and  $\Delta H$  is the height difference of the striking hammer (= initial height – upswing height). This energy loss, minus frictional losses, is considered to be the energy absorbed by the joint in the collision. When the bearing pad breaks from the sheath, energy loss accumulates along the joint. Therefore, the energy absorbed by the joint is normalized by joint length, to yield a measurement of impact strength in  $\text{J}\cdot\text{cm}^{-1}$ . The impact testing apparatus and sample holder are shown in Figure 2. Since the bearing pads feature chamfered edges, samples were cut in half to provide a vertical surface for the striking hammer to impact, encouraging the sample to break at the joint.

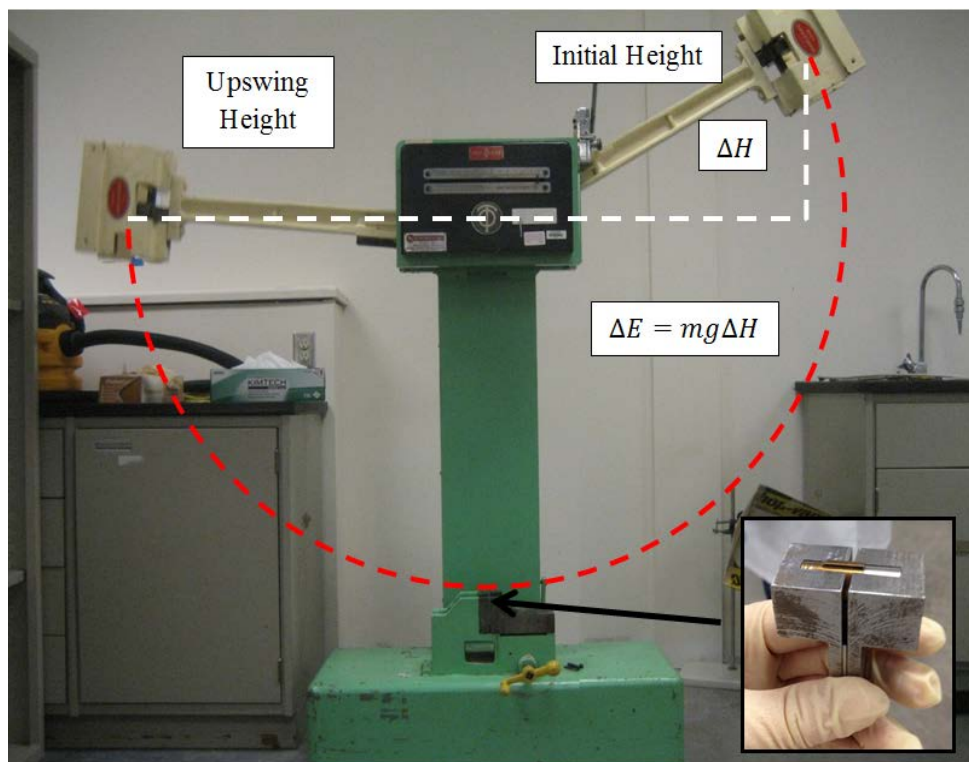


Figure 2- Impact testing apparatus. INSET: Bearing pad sample secured in sample holder.

## 2.2 Results and Discussion

Impact testing was performed on bearingpad samples brazed with Be and several replacement brazing materials. The replacement brazing material identities (labelled RB-1 to RB-4) are omitted here for proprietary reasons. Initially, this impact testing was performed on preliminary samples produced with materials RB-1 to RB-4 (hereafter referred to as “preliminary samples”), which were found to have lower impact strengths than those brazed with pure Be. Consequently, revised samples of RB-3 and

RB-4 were produced using different brazing parameters (*e.g.*, cycle time and temperature) in an attempt to increase their joint strengths.

Impact testing of bearing pad samples produced three distinct failure modes (Figure 3). Failure mode “A” is characterized by deformation of the bearing pad, which does not fracture from the brazed joint. Failure mode “B” is characterized by fracture of the bearing pad from the fuel sheath, with removal of the underlying sheath area. Failure mode “C” is characterized by fracture of the bearing pad from the sheath, with minimal deformation to the underlying sheath area.

Since the joint is not broken in failure mode “A”, these results are omitted from the braze joint average impact strength calculation. Conversely, since failure modes “B” and “C” are representative of joint strength, their results are grouped in calculating average impact strength (Figure 4). Since mode “B” has a larger variance than mode “C”, there is greater uncertainty in the average impact strengths of group having a greater propensity to fail via mode “B” (*i.e.*, Be, revised RB-3 and RB-4 groups).

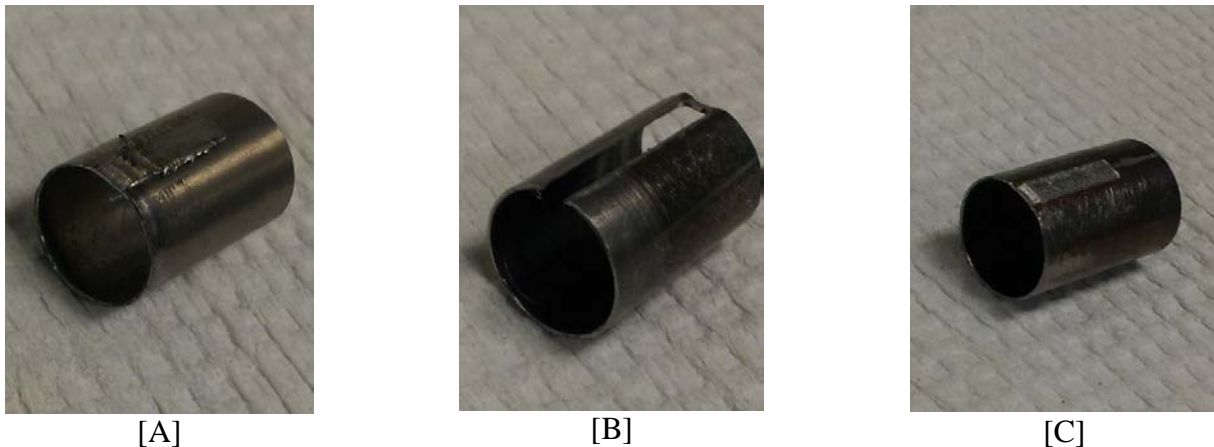


**Figure 3-Bearing pad impact testing failure modes: [A] Deformation of bearing pad; [B] Rough fracture of bearing pad from sheath; and [C] Peeling of bearing pad from sheath.**

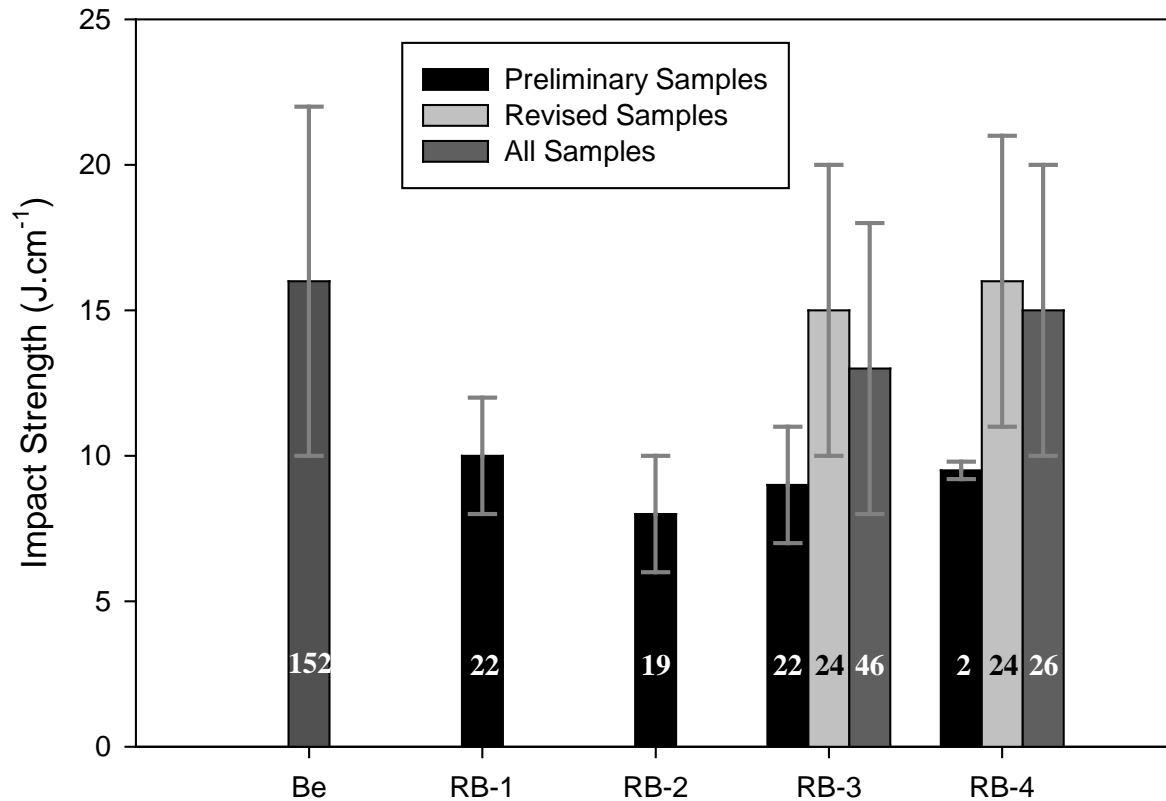


**Figure 4- Average impact strengths of beryllium and alternative materials, after correcting for friction loss. The average strengths of preliminary and revised sample groups are shown, as well as the total average strength. For RB-1 and RB-2, only preliminary samples were provided for testing. The number of samples tested in each group is indicated on each bar.**

Initial experiments were performed on Be-brazed joints to establish their impact strength, which will serve as a baseline comparator. Be-brazed joints yielded an average impact strength of  $16 \pm 6 \text{ J}\cdot\text{cm}^{-1}$ . Subsequently, the four *preliminary sample* groups (black bars, Figure 4) were found to have lower impact strengths than Be-brazed joints. Analysis of variance testing confirmed with high statistical significance that Be-brazed joints are stronger than the preliminary trials of RB-1, RB-2 and RB-3. However, for RB-4, the significance of this comparison was low as only two samples were available for preliminary testing.

In an attempt to increase joint strengths, additional samples of RB-3 and RB-4 were reproduced with revised brazing parameters (*e.g.*, brazing temperature and cycle time). It is noted that revised versions of RB-1 and RB-2 should be considered for future testing.

Modifying the brazing parameters increased the average impact strengths of revised samples to values comparable to the threshold impact strength ( $16 \pm 6 \text{ J}\cdot\text{cm}^{-1}$ ). The average impact strengths of the revised RB-3 and RB-4 groups are  $15 \pm 5 \text{ J}\cdot\text{cm}^{-1}$  and  $16 \pm 5 \text{ J}\cdot\text{cm}^{-1}$ , respectively. Analysis of variance

testing confirmed that neither of these groups had significantly different average impact strengths than the Be group. Results of these impact analyses will assist in the feasibility assessment of the candidate brazing materials and will be considered along with other data collected by the COG working group.

### 3. Modelling of Aqueous Solubility

Thermodynamic models may be used to predict the equilibrium solubility of metals in an aqueous system, at varying conditions of: (i) pH, (ii) reduction potential, (iii) pressure, and (iv) temperature. Using Gibbs Energy Minimization, the equilibrium phases present in the aqueous system may be calculated, allowing conditions of immunity, passivity, and corrosion susceptibility to be predicted. Models based upon the work of Pourbaix were developed to predict the corrosion behaviour of each alternative material alloy, in order to assist in determining each alloy's suitability for replacing beryllium as a filler material in CANDU brazed joints.

#### 3.1 Theory

Corrosion occurs by electrochemical processes, which are described by the generic reaction (Eq. 2), where  $R$  is a solid reactant,  $P$  is an ionic product in solution,  $H^+$  is the hydrogen ion in solution, and  $e^-$  are free electrons. The symbols  $r$ ,  $w$ ,  $x$ ,  $h$ , and  $n$  represent the reaction coefficients for the corresponding reactants and products.



The equilibrium reduction potential is given as a function of the activities of participating species by the Nernst equation (Eq. 3) [5]:

$$E = \frac{\Delta G}{nF} + \frac{0.0591}{n} \log \frac{(a_P)^x (a_{H^+})^h}{(a_R)^r (a_{H_2O})^w} \quad (3)$$

where  $E$  is the reduction potential,  $\Delta G$  is the standard free energy change of the reaction (Eq. 2),  $F$  is Faraday's constant,  $a$  is the activity of species involved, and  $n$  is the number of free electrons. It is noted that ionic activity is a measure of the "effective concentration" of an ion. Given that the activity of  $H_2O$  is necessarily equal to 1 (e.g.,  $a_{H_2O} = 1$ ), reactant  $R$  is solid (e.g.,  $a_R = 1$ ), and  $pH = -\log(a_{H^+})$ , the Nernst equation may be rewritten as:

$$E = \frac{\Delta G}{nF} + \frac{0.0591x}{n} \log(a_P) - \frac{0.0591h}{n} pH \quad (4)$$

This equation allows the equilibrium activity of ions in solution,  $a_P$ , to be calculated as a function of system pH and reduction potential, provided the Gibbs energy change of the dissolution reaction is known. The Gibbs energy change of the reaction is calculated as the sum of the Gibbs energy of formation ( $G_f$ ) of the products minus that of the reactants, which are determined at the specified temperature using Equation 5 [6]:

$$G_T = H_{298K}^o + \int_{298}^T C_P dT - T \left( S_{298K}^o + \int_{298}^T \frac{C_P}{T} dT \right) \quad (5)$$

Therefore, if standard thermodynamic data for the standard enthalpy of formation ( $H_{298K}^o$ ), entropy of formation ( $S_{298K}^o$ ), and constant pressure heat capacity ( $C_P$ ) are known, Equation 4 may be used to calculate the equilibrium activity of each possible species. At low ion concentrations ( $< 1 \times 10^{-4} \text{ mol L}^{-1}$ ), activity and concentration are approximately the same, and calculated activity is considered to be equivalent to the solubility limit for that ion [7].

### 3.2 Modelling Approach

To enable predictions of braze alloy solubility, a model containing thermodynamic data for possible braze alloy solid and aqueous species was established. A literature review was conducted to determine the enthalpy of formation, entropy of formation, and constant pressure heat capacity of the relevant solid and aqueous compounds of Zr, Be, Ni, Fe, and Cr, which comprise the significant constituents of the brazing alloys under consideration. The thermodynamic model was then validated by comparing Pourbaix diagrams produced to those published in the literature [8,9].

### 3.3 Preliminary Results

As an initial step in screening potential replacement brazing alloys, an assessment of corrosion resistance in conditions simulating a reactor shutdown is required. In these conditions, the coolant temperature is  $\sim 50^\circ\text{C}$  and the pH is near neutral ( $\sim 6.6$ ).

The aqueous speciation and equilibrium solubility of each significant brazing alloy element was calculated for these coolant conditions, using the developed model. Calculations were performed using FactSage thermochemical modelling software [10]. Results are shown below in Table 1.

**Table 1- Calculated solubility of relevant brazing alloy elements at  $50^\circ\text{C}$  and pH 6.6**

Braze Alloy Element	Predominant Aqueous Species	Calculated Solubility Limit ( $\text{mol L}^{-1}$ )
Zr	$\text{HZrO}_3[-]$	$4.90 \times 10^{-12}$
Be	$\text{Be}[2+]$	$1.31 \times 10^{-12}$
Fe	$\text{Fe}(\text{OH})_3$	$4.26 \times 10^{-12}$
Cr	$\text{Cr}(\text{OH})_3$	$3.29 \times 10^{-9}$
Ni	$\text{Ni}[2+]$	$4.00 \times 10^{-4}$

Noting that the boundary between solid and ionic species in Pourbaix diagrams is often taken to be  $1 \times 10^{-6} \text{ mol L}^{-1}$ , the aqueous solubility limit of the investigated brazing alloy elements was low (less than  $1 \times 10^{-8} \text{ mol L}^{-1}$ ), in all cases except for nickel, where a solubility limit of  $4.00 \times 10^{-4} \text{ mol L}^{-1}$  was calculated [8]. This indicates that in these conditions, dissolution of Zr, Be, Fe, and Cr is not thermodynamically favourable, but may be possible for Ni. However, it is noted that this preliminary model does not yet include multi-element compounds such as  $\text{NiFe}_2\text{O}_4$ , which are likely to be relevant

in mitigating corrosion in several candidate brazing alloys [11]. Work is currently ongoing to incorporate relevant multi-element compounds into the model.

Additionally, it is noted that the calculated solubility limits are equilibrium predictions, which do not necessarily represent the actual aqueous species concentrations in braze alloy systems. Depending on kinetics, a real system may not reach these predicted dissolved species concentrations. Therefore, experiments will be completed to compare real aqueous species concentrations to those predicted by the thermodynamic model.

#### **4. Corrosion Experiments**

In addition to modelling activities, experiments will be performed to investigate the corrosion resistance of alternative brazing materials at conditions characteristic of reactor shutdown. These are intended to support modelling predictions and to supplement the operational conditions testing performed by our project collaborators. An experiment apparatus has been designed, and experiments are currently underway.

##### **4.1 Experiment Set-up**

The *shutdown conditions* corrosion experiment is intended to simulate an extended reactor outage. Samples of bearing pad joints constructed with candidate materials will be exposed to water at 50°C, near neutral pH, and dissolved oxygen concentrations up to 3 ppm, for a period of 50 days. The bearing pad samples will then be removed, and properties including weight change, oxide thickness (on the braze alloy, bearing pad, and fuel sheath), hydrogen uptake (of the sheath and bearing pad), braze alloy degradation, and mechanical strength will be evaluated. These data will be used to assess potential corrosion effects on the integrities of the brazed joints and surrounding sheath areas.

An apparatus has been designed to accomplish this experiment (Figure 5 and Figure 6). The brazed joint specimens will be held in a Teflon sample holder, to keep samples electrically isolated from each other. The sample holder will sit in a sealed Pyrex vessel, containing an inert FEP (fluorinated ethylene propylene) liner to prevent test liquid contamination. Each sample type will be held in a vessel containing the test solution, and the vessels will be held in a temperature-controlled water bath for the duration of the experiment.



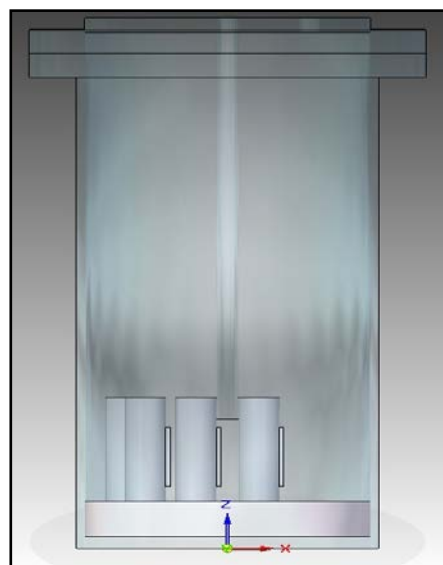


Figure 4- CAD model of the corrosion test apparatus.

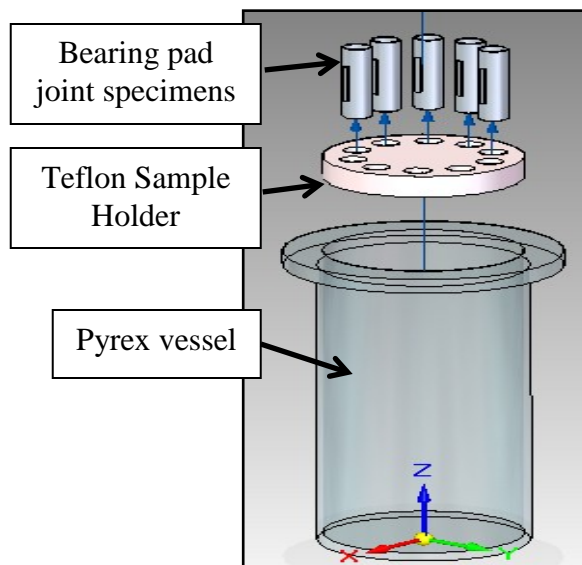


Figure 5- Exploded view of the test apparatus, showing the glass vessel, Teflon sample holder, and brazed bearing pad specimens.

After the experiment, inductively coupled plasma mass spectrometry (ICP-MS) analysis will be performed to measure the concentration of species that may have leached from the braze alloy into the test liquid. These results will be compared to aqueous species predictions from thermodynamic modelling activities.

## 5. Conclusions

A combination of impact testing, thermodynamic modelling, and corrosion experimentation is underway at the RMCC to assist in the suitability assessment of proposed Bereplacement brazing materials as part of a larger COG initiative.

The *preliminary samples* (RB-1 to RB-4) produced joints with lower impact strengths than Be-brazed joints. Recent samples of RB-3 and RB-4, produced by optimized brazing parameters, have comparable strength to current Be-brazed joints. RB-1 and RB-2 may produce stronger joints with improved brazing parameters; however, further investigation is required.

Corrosion studies of candidate brazing materials are proceeding. A preliminary thermodynamic model has indicated that the Ni present in some candidate brazing materials may dissolve in CANDU coolant at shutdown conditions, while other significant braze alloy elements have very low solubility limits and are unlikely to corrode ( $< 1 \times 10^{-8} \text{ mol L}^{-1}$ ). Work is ongoing to incorporate multi-element compounds into the model, which are likely to lower the modelled solubility of Ni at these conditions. Additionally, an experimental apparatus has been designed, and experiments are underway to support modelling predictions and assess the corrosion resistance of candidate braze joints in simulated reactor shutdown conditions.

## 6. Acknowledgements

The authors acknowledge the financial support of Natural Science and Engineering Research Council of Canada, the CANDU Owners' Group, and University Network of Excellence in Nuclear Engineering for financial support of this research effort. The authors are appreciative of the technical expertise and guidance from representatives of the Canadian Nuclear Laboratories (formerly AECL), Cameco Fuel Manufacturing, GE-Hitachi, Bruce Power, and Ontario Power Generation. These include R. Ham-Su, R. Harman, R. Scrannage, S. Palleck, T. Onderwater, E. Lu, and T. Daniels.

## 7. References

- [1] A. Manzer, "Introduction to CANDU Fuel", Presented to USNRC, Washington, DC. 4 September 2003. Available at <<http://pbadupws.nrc.gov/docs/ML0325/ML032530144.pdf>>
- [2] "Alert: Workplace Beryllium Exposure". Ontario Ministry of Labour, November 2010. Available at <<https://www.labour.gov.on.ca/english/hs/pubs/alerts/a21.php>>
- [3] E.C. Corcoran, T. Daniels, J. Harmsen, E. Lu, S. Palleck, A. Pant, T. Onderwater, and F. Dimayuga, "Status of The Beryllium Replacement Project", Presentation at the 12<sup>th</sup> International Conference on CANDU Fuel, Kingston, Ontario, Canada, 15-18 September 2013.
- [4] "ASTM D256: Standard Test Methods for Determining the Izod Pendulum Impact Resistance of Plastics", ASTM International, West Conshohocken, PA, 2010. Available at <[www.astm.org/Standards/D256.htm](http://www.astm.org/Standards/D256.htm)>
- [5] E.D. Verink, "Simplified procedure for constructing Pourbaix diagrams", *Uhlig's Corrosion Handbook*, Ch. 7, pp. 93-102, 2011.
- [6] M. Moran, H. Shapiro, D. Boettner, and M. Bailey, *Fundamentals of Engineering Thermodynamics*, John Wiley and Sons, 1 Dec, 2010.
- [7] S. Lower, "All About Electrochemistry: The Nernst Equation", Simon Fraser University 2012. Available at <<http://www.chem1.com/acad/webtext/elchem/ec4.html>>
- [8] M.H. Kaye and W.T. Thompson, "Computation of Pourbaix Diagrams at Elevated Temperatures", *Uhlig's Corrosion Handbook*, Ch. 9, pp. 111-122, 2011.
- [9] B. Beverskog and I. Puigdomenech, "Revised Pourbaix Diagrams for Nickel at 25-300 °C", *Corrosion Science*, Vol. 39, 1997.
- [10] C.W. Bale, E. Bélisle, P. Chartrand, S.A. Decterov, G. Eriksson, K. Hack, I.H. Jung, Y.B. Kang, J. Melançon, A.D. Pelton, C. Robelin, and S. Petersen, "FactSage Thermochemical Software and Databases - Recent Developments", *Calphad*, vol. 33, pp. 295-311, 2009.<[www.factsage.com](http://www.factsage.com)>

- [11] W.T. Thompson, M.H. Kaye, C.W. Bale, and A.D. Pelton, “Pourbaix Diagram Construction for Multi-element Systems”, *Uhlig's Corrosion Handbook*, Ch. 8, pp. 103-110, 2011.